

Analysis of Results of High-Energy Nuclear Reactions*

NORBERT T. PORILE† AND NATHAN SUGARMAN

Enrico Fermi Institute for Nuclear Studies and Department of Chemistry, University of Chicago, Chicago, Illinois

(Received May 28, 1957)

The determination of branching ratios for the formation of specific products at given deposition energies is described for high-energy nuclear reactions. These branching ratios may be obtained by use of deposition energy spectra from recent Monte Carlo calculations. The calculated branching ratios are used to analyze formation cross sections in the Bev region into "fission" and "fragmentation" components, and to calculate average and most probable deposition energies for the formation of specific nuclides. The fission process in bismuth is compared with that in tantalum as to relative fissionability, deposition energy for fission, and spread in fissioning nuclei.

I. INTRODUCTION

NUCLEAR reactions induced by particles with incident energies above 70 or 80 Mev are best described in terms of the "cascade-evaporation" model first suggested by Serber.¹ At these energies, where the mean free path of the incident particle becomes comparable to nuclear dimensions, the target nucleus appears as a partially transparent collection of quasi-free nucleons to the incoming particle. The cascade process consists of two-body collisions between the incident particle and the nucleons of the target nucleus, and subsequent collisions of the struck nucleons, which results in the emission of "knock-on" particles. The nuclear cascades leave the residual nucleus in various states of excitation, up to the excitation produced by the deposition of all the incident energy. The excitation energy is then dissipated by the subsequent evaporation of particles, much in the same way as in low-energy bombardments. The observed nuclear reactions are thus the result of a variety of processes representing the deposition of different amounts of excitation energy.

There is a parallelism in the quantitative treatment of cross-section data from high-energy reactions and low-energy reactions involving compound-nucleus formation. In the case of the latter, the cross section for forming a given product A , σ_A , is given by the product of the cross section for forming the compound nucleus and the branching ratio of the excited compound nucleus to A . Similarly, in the case of high-energy reactions, σ_A is the integral for all values of the excitation energy E^* of the product of the cross section for forming a residual nucleus with a given E^* , and the branching ratio of the decay into A for that excitation energy. The cross section for forming a nucleus with excitation energy E^* is given by the product of the geometric cross section of the target nucleus, σ_g , and the probability that a projectile of energy E_p will deposit excitation energy E^* , $N(E^*, E_p)$. The expression for the

observed cross section for forming a product A at a bombarding energy, E_p , for a given target nucleus, is given in

$$\sigma_A(E_p) = \int_0^{E_{\max}^*} \sigma_g \times N(E^*, E_p) \times f_A(E^*) dE^*, \quad (1)$$

Eq. (1), where E_{\max}^* is the maximum excitation energy that may be deposited, corresponding to the sum of the kinetic and binding energies of the bombarding particle, and $f_A(E^*)$ is the branching ratio for the residual nucleus with excitation energy E^* for formation of A . There will, in general, be a different $f_A(E^*)$ for each residual nucleus formed with a given excitation energy. In Eq. (1), $f_A(E^*)$ is the average branching ratio for all such residual nuclei. It is noted that $f_A(E^*)$ has been assumed to be independent of the bombarding energy. In Eq. (1), $N(E^*, E_p)$ is normalized so that its integral over E^* is unity. The nuclear radius has been taken as $1.3 \times 10^{-13} A^{1/2}$ cm for calculation of the geometric cross sections of the target nuclei, the value used in the Monte Carlo calculations.²

The quantity $f_A(E^*)$ is of interest in high-energy reactions since it represents the probability for forming a given product, not at a given bombarding energy, but at a given deposition energy, thereby providing specific information on the relative contributions of different parts of the deposition energy spectrum to the observed cross section. Values of $f_A(E^*)$ may be obtained from observed excitation functions by use of Eq. (1) and the deposition energy spectra $N(E^*, E_p)$ for all values of E_p for which there are cross-section data. Recent Monte Carlo calculations² have made available deposition energy spectra for a number of target elements for a wide range of bombarding energies. These results may thus be combined with experimentally measured excitation functions,³⁻⁶ to yield the desired branching

* This work was supported in part by a grant from the U. S. Atomic Energy Commission.

† Presented in partial fulfillment of the Ph.D. degree in the Department of Chemistry, University of Chicago. The author acknowledges the aid of General Electric and National Science Foundation fellowships. Now at Brookhaven National Laboratory, Upton, New York.

¹ R. Serber, *Phys. Rev.* **72**, 1114 (1947).

² A. Turkevich, University of Chicago (private communication). Some of these results have been briefly reported on: Bivins, Metropolis, Storm, Turkevich, Miller, and Friedlander, *Bull. Am. Phys. Soc. Ser. II*, **2**, 63 (1957).

³ L. Jodra and N. Sugarman, *Phys. Rev.* **99**, 1470 (1955).

⁴ Wolfgang, Baker, Caretto, Cumming, Friedlander, and Hudis, *Phys. Rev.* **103**, 394 (1956).

⁵ H. M. Steiner and J. A. Jungerman, *Phys. Rev.* **101**, 807 (1956).

⁶ E. L. Kelly and C. Wiegand, *Phys. Rev.* **73**, 1135 (1948).

ratios, $f_A(E^*)$. Analyses of spallation and fission data for a given bombarding energy have previously been made by Meadows,⁷ Jackson,⁸ Russell,⁹ and Rudstam,¹⁰ by use of Monte Carlo calculations. In this study we restrict ourselves to reactions of bismuth, lead, and tantalum with protons, giving products in the "fission" region. The $f_A(E^*)$ values are calculated for several typical cases, and are used to interpret cross-section data, to calculate deposition energies for formation of specific fission products, and to compare the high-energy fission process in bismuth with that in tantalum.

II. DETERMINATION OF THE BRANCHING RATIO, $f_A(E^*)$

The branching ratio for forming a product A at a deposition energy E^* , $f_A(E^*)$, may be obtained from the measured excitation functions and the deposition energy spectra by use of Eq. (1). The problem here is formally analogous to the calculation of cross sections in photonuclear reactions from the observed yields at maximum bremsstrahlung energies. In this study, the $f_A(E^*)$ curves were obtained by trial and error. Successive adjustments were made to the assumed $f_A(E^*)$

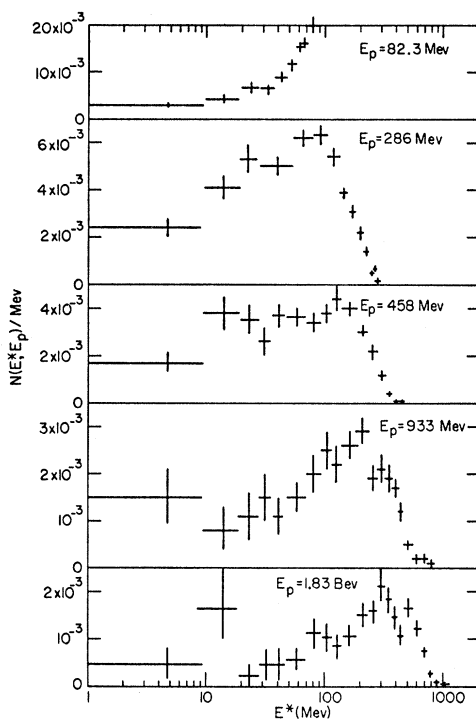


FIG. 1. Deposition energy spectra obtained for proton bombardment of bismuth from Monte Carlo calculations. The tabulated deposition energy intervals and the statistical error associated with each value are indicated by the crosses.

⁷ J. Meadows, Phys. Rev. **98**, 744 (1955).

⁸ J. D. Jackson, Can. J. Phys. **34**, 767 (1956); **35**, 21 (1957).

⁹ I. J. Russell, Ph.D. thesis, University of Chicago, 1956 (unpublished).

¹⁰ G. Rudstam, "Spallation of Medium Weight Elements," Uppsala 1956, Appelbergs, Boktryckeri Ab.

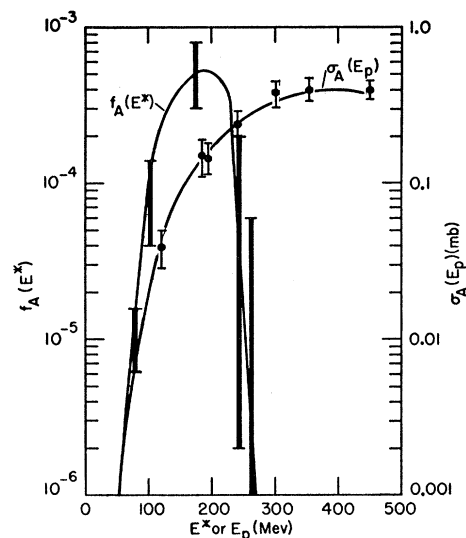


FIG. 2. Variation of $f_A(E^*)$ with E^* and of $\sigma_A(E_p)$ with E_p for Cu^{67} from proton bombardment of bismuth.

curve until it was able to reproduce the observed $\sigma_A(E_p)$ values to within about 2%. The deposition energy spectra for proton bombardment of bismuth used in this determination were obtained from the Monte Carlo calculations,² and are shown in Fig. 1. The statistical errors associated with the calculated values are given.

The resulting curve of $f_A(E^*)$ vs E^* is shown for two typical cases in Figs. 2 and 3. In Fig. 2, the $f_A(E^*)$ curve for Cu^{67} formed in the proton bombardment of bismuth is given for deposition energies up to 450 Mev. The measured excitation function for Cu^{67} ,³ $\sigma_A(E_p)$ vs E_p , used to obtain the $f_A(E^*)$ curve is also included. It is seen that the $f_A(E^*)$ curve initially rises more steeply than the corresponding $\sigma_A(E_p)$ curve, and then, as the latter begins to flatten, goes through a maximum and decreases sharply. This general behavior is characteristic of $f_A(E^*)$ curves associated with excitation functions that become flat or go through a maximum at bombarding energies below 500 Mev. The errors associated with the derived $f_A(E^*)$ curve for Cu^{67} are indicated by the heavy vertical bars in Fig. 2. These are the maximum expected errors, obtained by assuming a pileup of the errors in $N(E^*, E_p)$ and $\sigma_A(E_p)$. The maximum error is about 50 to 60% for deposition energies less than 200 Mev. In the region beyond the maximum of the $f_A(E^*)$ curve, the errors become very large, and the $f_A(E^*)$ values are known only to within a factor of 10 or 20. In spite of this large uncertainty, however, it is apparent that $f_A(E^*)$ actually does go through a rather sharp maximum. The large uncertainty in $f_A(E^*)$ at deposition energies close to the maximum bombarding energy arises from the fact that $N(E^*, E_p)$ is very small for E^* close to E_p . Hence, the product of $N(E^*, E_p)$ and $f_A(E^*)$ will make a rather small con-

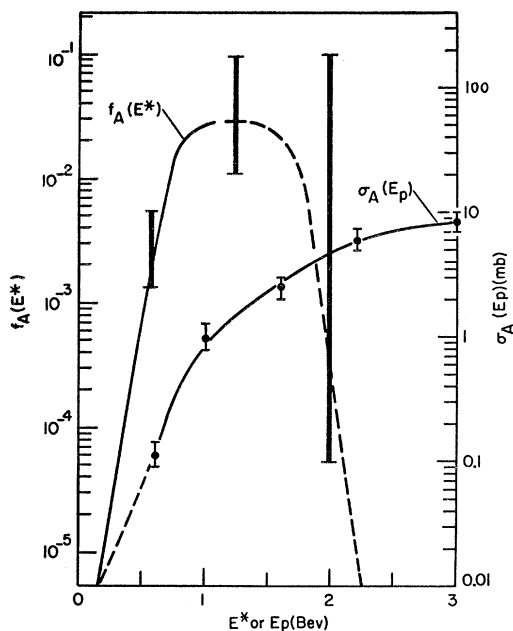


FIG. 3. Variation of $f_A(E^*)$ with E^* and of $\sigma_A(E_p)$ with E_p for Ba^{131} from proton bombardment of lead.

tribution to the observed cross section, $\sigma_A(E_p)$, regardless of the value of $f_A(E^*)$ within fairly wide limits. Also, the statistical uncertainty in $N(E^*, E_p)$ is very large for E^* close to E_p , due to the small number of cascades leading to large E^* values.

In Fig. 3 we have plotted the $f_A(E^*)$ curve for Ba^{131} formed in proton bombardment of lead up to 3 Bev, as well as the corresponding excitation function.⁴ The $f_A(E^*)$ curve can actually only be calculated to E^* values of about 1 Bev, since, for the 1.83 Bev cascade calculations,² out of a total of nearly 600 cascades none leading to E^* values above 1.2 Bev were observed. The dashed continuation of the $f_A(E^*)$ curve for Ba^{131} above 1 Bev was obtained on the assumption that there were actually two events leading to E^* greater than 1.2 Bev. A different choice for $N(E^*, E_p)$ would lead to a different shape for the $f_A(E^*)$ curve. The very large errors indicated in Fig. 3 reflect this situation. The errors have been terminated at $f_A(E^*)$ values of 0.1. This reflects our belief that the branching ratio, at a given E^* value, for any product will not be more than 10%. The $f_A(E^*)$ curve consequently levels off, and possibly goes through a maximum, as indicated in Fig. 3.

There are three differences between the $f_A(E^*)$ curves for Cu^{67} and Ba^{131} . These may be correlated with the fact that the excitation function for Cu^{67} flattens below 500 Mev, whereas the excitation function for Ba^{131} only begins to flatten near 3 Bev. First, the $f_A(E^*)$ curve for Cu^{67} goes through a maximum, while the corresponding curve for Ba^{131} may or may not go through a maximum. For 500-Mev bombarding energy, $N(E^*, E_p)$ is small, but still with a value of about a few

percent, for E^* close to E_p . Hence, if the excitation function goes through a maximum, $f_A(E^*)$ has to go through a rather sharp maximum so that the higher deposition energy processes do not contribute substantially to the observed cross section. This behavior of the branching ratio has also been found by Russell⁹ in his analysis of the pion- and proton-induced fission of uranium. In the Bev region, on the other hand, $N(E^*, E_p)$ is very close to zero for E^* close to E_p . Consequently the excitation function can flatten or go through a maximum without necessarily requiring $f_A(E^*)$ to go through a maximum.

Second, the ratio of the maximum value of $f_A(E^*)$ to the maximum value of $\sigma_A(E_p)$ is greater for Ba^{131} than for Cu^{67} . This observation once again reflects the fact that the fraction of cascades leading to deposition energies in the Bev region, for incident energies of 1 to 3 Bev is very small. Consequently the corresponding $f_A(E^*)$ values are rather large, in order to account for the substantial cross section observed in the Bev region. Third, the absolute width at half-maximum of the $f_A(E^*)$ curve for Ba^{131} is much greater than that of the corresponding curve for Cu^{67} , indicating formation of Ba^{131} over a wider deposition energy region.

III. FISSION AND FRAGMENTATION

The analysis of the excitation function for Cu^{67} , given in Fig. 2, shows that the production of Cu^{67} with 450-Mev protons arises from deposition energies below 270 Mev. It is of interest to determine whether this low-energy process accounts for the entire cross section for making Cu^{67} in the Bev region, or whether in addition, one has to invoke contributions from a higher energy process. Assuming that the former is true, we may by use of Eq. (1) calculate an excitation function for Cu^{67} to 3 Bev. For this purpose it is convenient to approximate the $f_A(E^*)$ curve for Cu^{67} by a rectangle, centered at 180 Mev, 150-Mev wide and with a value of 3×10^{-4} . In this case, then, $\sigma_A(E_p)$ depends upon the integral of $N(E^*, E_p)$ for deposition energies between 105 and 255 Mev at each bombarding energy. We have previously assumed that $f_A(E^*)$ does not depend on the bombarding energy. This assumption may not be strictly true, however, particularly over the wide range in bombarding energies under consideration. The branching ratio $f_A(E^*)$ is, as was previously stated, an average of the branching ratios for all the residual nuclei resulting from the cascade process leading to the same deposition energy. The average branching ratio will thus be independent of bombarding energy only if the distribution in residual nuclei for a given deposition energy is independent of bombarding energy. An examination of the Monte Carlo cascades² shows that in going from 458-Mev to 1.83-Bev bombarding energy the average number of nucleons emitted from cascades in bismuth leading to deposition energies of about 170 Mev increases from about 3 at 458 Mev to about 6 at

1.83 Bev and that Z^2/A of the average residual nucleus decreases from 33.2 to 32.7. It may be expected that $f_A(E^*)$ will decrease with increasing bombarding energy, since the residual nuclei become, on the average, less fissionable. The magnitude of this effect can be estimated from the observed dependence of the production cross sections of fission products on the charge and mass of the target nucleus in 450-Mev proton bombardments.¹¹ The correction to the $f_A(E^*)$ values at 3-Bev bombarding energy, obtained from excitation functions to 450 Mev, is greatest for symmetric fission products where it amounts to a reduction by a factor of two or three, whereas for Cu⁶⁷ it amounts to a reduction of about 20%. This difference is due to the broadening of the fission yield curve observed in going to targets of lower Z .¹¹

We assume that the $f_A(E^*)$ rectangle, although varying in height, does not shift appreciably in deposition energy with increasing bombarding energy. A large shift in deposition energy would affect the values of the integral of $N(E^*, E_p)$, and thereby the values of $\sigma_A(E_p)$. Our justification for this assumption is that the average E^* value for the production of a given fragment in the fission of bismuth with 450-Mev protons is only slightly lower than that in tantalum.¹² Since the difference in Z^2/A under consideration for the residual nuclei resulting from the bombardment of bismuth with protons of different energy is much smaller than that of corresponding residual nuclei for bismuth and tantalum at 450 Mev, we may expect that there will be no significant shift of the $f_A(E^*)$ rectangle along the E^* axis.

The cross section of Cu⁶⁷ from bismuth was calculated to 3-Bev bombarding energy on the basis of data up to 450 Mev, in the manner outlined above. The $\sigma_A(E_p)$ values obtained by use of Eq. (1) were corrected at each energy for the decrease in $f_A(E^*)$ by multiplication by a correction function obtained by interpolation from the Monte Carlo data at several energies and from the fission yield studies at 450 Mev.¹¹ The resulting excitation function for Cu⁶⁷ is plotted in Fig. 4. The error at each bombarding energy is primarily the error associated with $N(E^*, E_p)$ at E^* between 105 and 255 Mev for the same bombarding energy. The points are the experimentally observed cross sections obtained at Brookhaven for proton bombardments of lead.⁴ The Chicago data were normalized to the Brookhaven data at 400 Mev by increasing the Chicago values by a factor of 2.1. The origin of this discrepancy may be due to different corrections for counting efficiency of the weak β radiation of Cu⁶⁷. The height of the $f_A(E^*)$ rectangle was increased by the same factor. We assume that there will be no significant change in position of the $f_A(E^*)$ rectangle along the E^* axis in going from bismuth to lead. It is seen that the predicted cross

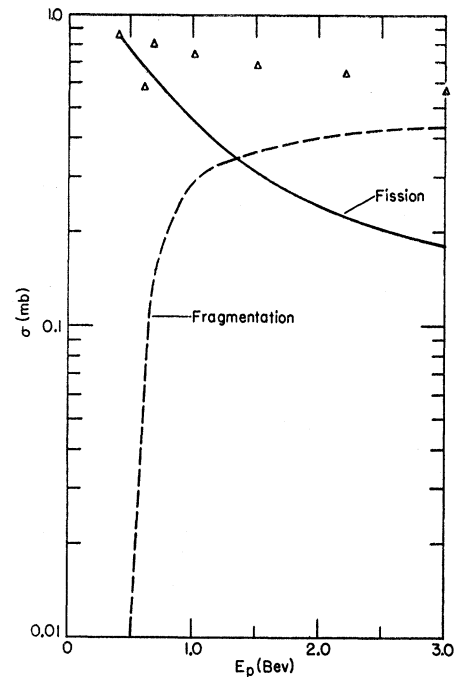


FIG. 4. Comparison of experimental and calculated $\sigma_A(E_p)$ curves for Cu⁶⁷ from proton bombardment of lead. The Δ symbols are the experimental values of Wolfgang, *et al.*⁴ Solid curve—calculated “fission” cross section. Dashed curve—calculated “fragmentation” cross section.

section in the Bev region is considerably smaller than the experimental value. This suggests that there is a contribution to the observed cross section in the Bev region from a high deposition energy process, in addition to the low deposition energy process responsible for the observed cross section at lower bombarding energies. We shall refer to this low deposition energy process as “fission” and to the suggested high deposition energy process as “fragmentation.” We use the term “fragmentation” in the same sense as Wolfgang *et al.*,⁴ namely, as a high deposition energy process associated with pion formation and readsorption. It is possible to determine the relative contribution of each process to the observed cross section at any bombarding energy by subtracting the calculated “fission” cross section from the observed cross section. The resulting excitation function for the “fragmentation” process is given by the dashed line in Fig. 4. It is seen that the “fragmentation” cross section becomes comparable to the “fission” cross section at 1.3 Bev and predominates at higher energies. This fragmentation excitation function may be analyzed to yield an $f_A(E^*)$ curve by the use of Eq. (1). The resulting curve has the same general appearance as the $f_A(E^*)$ curve for Ba¹³¹, with a maximum value of about 4×10^{-3} at 1.1 Bev and a width at half-maximum of approximately 700 Mev. As in the case of Ba¹³¹, the uncertain value of $N(E^*, E_p)$ above 1 Bev may lead to substantial errors in $f_A(E^*)$. If the excitation function for Cu⁶⁷ is not divided into two energy intervals, each

¹¹ P. Kruger and N. Sugarman, *Phys. Rev.* **99**, 1459 (1955).

¹² N. T. Porile and N. Sugarman, preceding paper [*Phys. Rev.* **107**, 1410 (1957)].

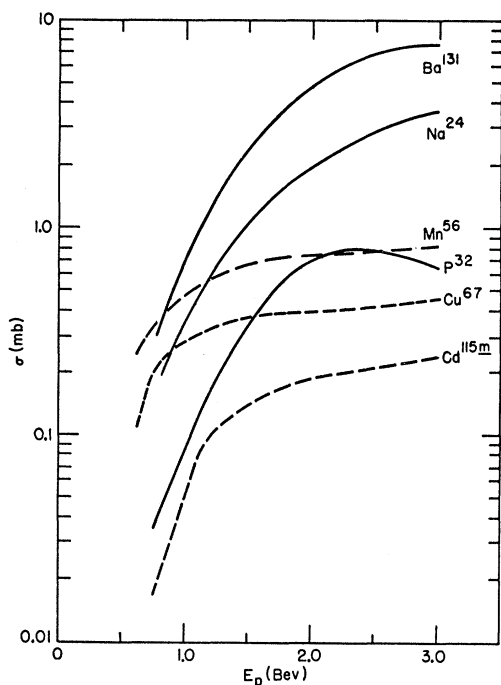


FIG. 5. Excitation functions for "fragmentation" process. Solid curves—experimental excitation functions obtained by Wolfgang, *et al.*⁴ Dashed curves—calculated "fragmentation" excitation functions.

of which is analyzed separately, but is treated as one continuous function, it is still necessary to assume the presence of at least two peaks in the $f_A(E^*)$ curve in order to reproduce the observed $\sigma_A(E_p)$ values. An $f_A(E^*)$ curve with only one peak, centered perhaps at 500 or 600 Mev does not fit the data.

The calculation described for Cu^{67} was repeated for Mn^{56} and Cd^{115m} , the two other nuclides for which there are both low- and high-energy data available. The position of the low-energy $f_A(E^*)$ rectangle was obtained from average deposition energies obtained in recoil studies of bismuth fission with 450-Mev protons.^{12,13} The relation between the average deposition energy and $f_A(E^*)$ is described in the following section. The deposition energy data was used since no excitation functions up to 450 Mev were available for these nuclides. The $f_A(E^*)$ rectangles for Mn^{56} and Cd^{115m} were centered at 195 Mev and 160 Mev, respectively, and were adjusted in height so that the calculated cross sections agreed with the values obtained by Wolfgang *et al.*⁴ at 450 Mev. In the case of Mn^{56} the experimental values had to be extrapolated down to 450 Mev to permit the normalization. The width of the $f_A(E^*)$ rectangles could be varied between 50 and 250 Mev with negligible results on the calculated cross section values. Consequently it was not necessary to obtain a well-defined value for the width of the $f_A(E^*)$ rectangles. The lowering of the height of the $f_A(E^*)$

¹³ N. T. Porile (unpublished results).

rectangle in 3-Bev bombardments relative to the height for 450-Mev bombardments was found to be negligible in the case of Mn^{56} , and amounted to a factor of 2.6 for Cd^{115m} . Just as in the case of Cu^{67} it was found necessary to postulate contributions from the "fragmentation" process for both nuclides in order to explain the difference between the observed and calculated values.

The excitation functions for the calculated fragmentation components of Mn^{56} , Cu^{67} , and Cd^{115m} are plotted in Fig. 5. The excitation functions for a number of light nuclides have been determined in bombardments of lead by Wolfgang and co-workers.⁴ These nuclides, such as Na^{24} or P^{32} , are made in very low yield at 600 Mev and their excitation functions show a behavior consistent with a high deposition energy fragmentation process. The measured excitation functions for Na^{24} and P^{32} , as well as for Ba^{131} , are included in Fig. 5. It can be seen that the calculated fragmentation curves have about the same shape and magnitude as the experimental curves. Fragmentation thus appears to lead to products over the whole mass region, as was pointed out by Wolfgang *et al.*⁴ Our analysis indicates that at 3 Bev the fragmentation cross sections are lowest for products of roughly half the mass of the target nucleus and increase by about an order of magnitude for the lightest observed nuclides. A similar increase is seen in the heavy mass region, as evidenced by Ba^{131} , but the situation is complicated by the contribution from the spallation process in this mass region. The analysis of the observed cross sections into their "fission" and "fragmentation" components indicates that the total "fission" cross section at 3 Bev for lead or bismuth is down by about a factor of 5 to 10 from its value at 450 Mev, to a value of 20 to 40 millibarns.

IV. DEPOSITION ENERGY

The $f_A(E^*)$ curves may be used to calculate, for each bombarding energy, the average value of the excitation energy deposited in the struck nucleus for processes leading to fragment A , denoted by \bar{E}_A^* . This quantity is given by Eq. (2):

$$\bar{E}_A^* = \frac{\int_0^{E_{\max}^*} E^* \times \sigma_g \times N(E^*, E_p) \times f_A(E^*) dE^*}{\int_0^{E_{\max}^*} \sigma_g \times N(E^*, E_p) \times f_A(E^*) dE^*} \quad (2)$$

Figure 6 shows the values of \bar{E}_A^* for Ba^{131} , Cu^{67} , and a hypothetical fragment X from bismuth up to a bombarding energy of 1 Bev. Fragment X is made exclusively by a low-energy process. The \bar{E}_A^* curve for fragment X essentially levels off at rather low bombarding energies. The curve for Cu^{67} shows an initial rise followed by a plateau and another rise, reflecting

the high deposition energy process. The curve for Ba^{131} increases monotonically, as does the corresponding $f_A(E^*)$ curve to 1 Bev. It is thus clear that the experimental determination of average deposition energies for various bombarding energies can be of considerable value in differentiating between different kinds of formation processes.

Deposition energy values can be obtained directly, independent of the above considerations, from recoil studies.¹²⁻¹⁵ One obtains from the latter the forward component of momentum imparted to the struck nucleus. The deposition energies may then be obtained from the momentum values with the aid of a momentum-deposition energy relation obtained from the Monte Carlo calculations.² This relation, Fig. 4 of the preceding paper,¹² was obtained on the assumption that a given fragment is formed from nuclei of a given excitation energy. The breadth of the $f_A(E^*)$ curves shows that this is not the case. A correct treatment gives the average forward component of momentum imparted to the struck nucleus for formation of fragment A , \bar{P}_A , by the equation:

$$\bar{P}_A = \frac{\int_0^{E_{\max}^*} \bar{P}(E^*, E_p) \times \sigma_\theta \times N(E^*, E_p) \times f_A(E^*) dE^*}{\int_0^{E_{\max}^*} \sigma_\theta \times N(E^*, E_p) \times f_A(E^*) dE^*}, \quad (3)$$

where $\bar{P}(E^*, E_p)$ is the average momentum imparted to the struck nucleus corresponding to a given deposition energy E^* for a bombarding energy E_p . $\bar{P}(E^*, E_p)$ is the quantity that is actually plotted against E^* in Fig. 4 of the preceding paper. In order to obtain values of \bar{E}_A^* from the measured values of \bar{P}_A it is thus necessary to correct for the width of the $f_A(E^*)$ curve. Increasing the width of the latter from 0 to 200 Mev raises the corresponding value of \bar{E}_A^* for a given \bar{P}_A by a few Mev from that given in Fig. 4 of the preceding paper.

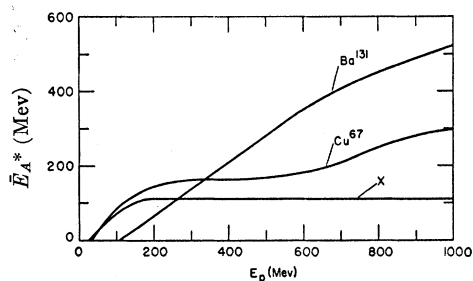


FIG. 6. Variation of \bar{E}_A^* with E_p for Ba^{131} , Cu^{67} , and a hypothetical fragment X formed in proton bombardment of bismuth.

¹⁴ Sugarman, Campos, and Wielgoz, *Phys. Rev.* **101**, 388 (1956).

¹⁵ Perfilov, Ivanova, Lozhkin, Ostroumov, and Shamov, *Proceedings of the Conference of the Academy of Sciences of the U.S.S.R. on the Peaceful Uses of Atomic Energy, Moscow, July 1, 1955* (Akademiiia Nauk, S.S.S.R., Moscow, 1955), p. 55 [translated by Consultants Bureau, New York (1955)].

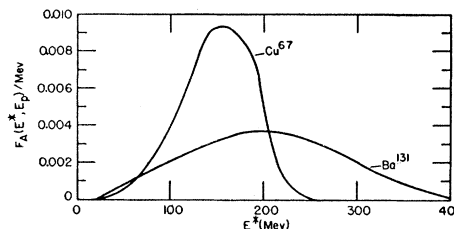


FIG. 7. Variation of $F_A(E^*, E_p)$ with E^* for Cu^{67} and Ba^{131} in 400-Mev proton bombardment of bismuth.

Equation (3) may be used directly to obtain values of the average forward component of momentum of the struck nucleus from the experimentally determined excitation functions through the use of the Monte Carlo calculations,² as discussed earlier. The excitation-function data for Cu^{67} ³ give a value of 0.516 in units of 931 Mev/c for \bar{P}_A , in 450-Mev proton bombardment of bismuth. This value is in excellent agreement with the value of 0.528 ± 0.009 obtained from recoil studies.¹²

The most probable deposition energy required to form a given nuclide may be obtained for a given bombarding energy by plotting the quantity $\sigma_\theta \times N(E^*, E_p) \times f_A(E^*)$ versus E^* , and noting the position of the maximum. If this expression is divided by the value of the measured cross section of the nuclide at the desired bombarding energy, $\sigma_A(E_p)$, the quantity obtained is

$$F_A(E^*, E_p) = \frac{\sigma_\theta \times N(E^*, E_p) \times f_A(E^*)}{\sigma_A(E_p)}$$

$F_A(E^*, E_p)$ represents the fractional contribution to the total cross section of A for a bombarding energy E_p by nuclei of deposition energy E^* . A plot of $F_A(E^*, E_p)$ for Cu^{67} and Ba^{131} calculated for 400-Mev proton bombardment of bismuth is given in Fig. 7. It can be seen that the Cu^{67} fragments originate in the main from a narrower deposition energy interval than the Ba^{131} fragments. This result is a consequence of the fact that the $f_A(E^*)$ curve for Ba^{131} is still rising sharply at E^* of 400 Mev (see Fig. 3) so that the product of $f_A(E^*)$ and $N(E^*, E_p)$ is fairly constant despite the decrease in the $N(E^*, E_p)$ curve above 150 Mev. For Cu^{67} , on the other hand, both curves decrease above E^* values of 200 Mev, and hence the $F_A(E^*, E_p)$ curve decreases sharply. In the model of the "fissioning nucleus" this means that the approximation of a single fissioning nucleus is better for processes leading to Cu^{67} than to Ba^{131} , although even for the former, the most probable fissioning nucleus only gives rise to about 10% of the total yield in 400-Mev bombardments.

V. FISSION PROCESS IN BISMUTH AND TANTALUM

The analysis of excitation functions by use of Monte Carlo calculations presented earlier may be applied to the case of the total fission cross section of bismuth^{3,5,6} and tantalum. The excitation function for tantalum may

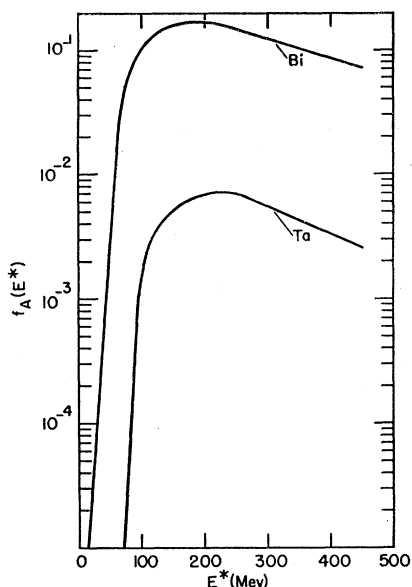


FIG. 8. Variation of $f_A(E^*)$ with E^* for proton fission of bismuth and tantalum.

be obtained by extrapolation from measured values for bismuth and gold,⁵ combined with measurements of the total fission cross section of tantalum at individual energies.^{11,16} The resulting $f_A(E^*)$ ¹⁷ curves are plotted to E^* values of 450 Mev in Fig. 8. Both curves go through a maximum and the decrease beyond the maximum is less sharp than that observed for individual fission fragments (see Fig. 2), since these curves for the fission process represent the total of many individual $f_A(E^*)$ curves, peaked at different energies. Several conclusions may be drawn from these curves. First, the branching ratio for fission in bismuth attains a peak value of 0.17 at a deposition energy of 190 Mev, and then decreases. The maximum value for the branching ratio for fission of tantalum is 0.007 at a deposition energy of 230 Mev. At no deposition energy is fission the predominating process for either bismuth or tantalum.

Second, the fact that the $f_A(E^*)$ curves for fission go through a maximum, coupled with the fact that the $N(E^*, E_p)$ curves also go through a maximum for all bombarding energies for which there are data,² implies that the corresponding excitation functions go through a maximum. This maximum in the excitation function for fission will occur at a bombarding energy for which the most probable deposition energy is about equal to the deposition energy corresponding to the maximum in the $f_A(E^*)$ curve. With the aid of the deposition energy spectra we estimate this bombarding energy to be about 750 Mev for bismuth, and 1.5 Bev for tantalum.

Third, the ratio of the integral of $f_A(E^*)$ for E^* values between 0 and 450 Mev for bismuth to that for

tantalum is about 30. This is the calculated ratio of the 450-Mev fission cross sections of bismuth and tantalum, on the assumption that $N(E^*, E_p)$ has a constant value for all deposition energies. This ratio of 30 then represents what might be called the greater "intrinsic" fissionability of bismuth. The ratio of the observed fission cross section of bismuth and tantalum at 450 Mev, is about 44.¹¹ There is, then, an extra factor of about 1.5 favoring the fission of bismuth over that of tantalum, in 450-Mev bombardments, besides the factor of 30 obtained from the branching ratios. This extra factor comes from the fact that the average deposition energy for all inelastic events is closer to the deposition energy corresponding to the maximum in the $f_A(E^*)$ curve for bismuth than for tantalum.

The results of recent recoil studies on fission products from bismuth and tantalum with 450-Mev protons¹² show that there is no marked dependence of the average deposition energy on the mass asymmetry of the most probable fragments. The preference for symmetric fission found in high-energy bombardment of these elements¹¹ is consequently inherent in the fission act itself.

The average and most probable deposition energies for the fission of bismuth and tantalum may be obtained as a function of bombarding energy to 450 Mev. The resulting curves are shown in Figs. 9 and 10 for bismuth and tantalum, respectively. We include for comparison a plot of the average deposition energy for all inelastic events, obtained from the Monte Carlo calculations.² At the very lowest bombarding energies, where the compound-nucleus model is applicable, all three quantities coincide. At higher bombarding energies, the \bar{E}^* values for fission are higher than those for all inelastic

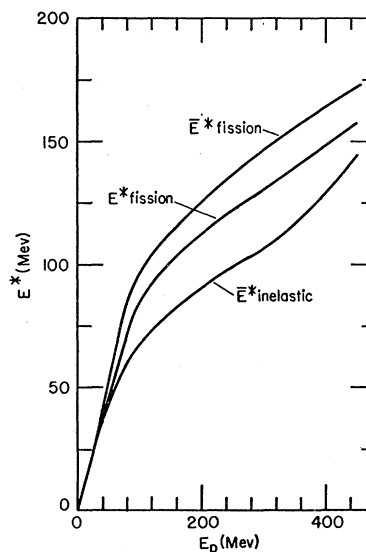


FIG. 9. Variation of deposition energy with bombarding energy for bismuth. \bar{E}^* fission—average deposition energy for fission. E^* fission—most probable deposition energy for fission. \bar{E}^* inelastic—average deposition energy for all inelastic events.

¹⁶ W. E. Nervi and G. T. Seaborg, Phys. Rev. **97**, 1092 (1955).

¹⁷ The subscript A now refers to the fission process in general rather than to the formation of a specific product.

events, a consequence of the very low branching ratios for fission at low deposition energies (see Fig. 8), particularly in the case of tantalum. Higher values of \bar{E}^* are obtained for the fission of tantalum as compared to bismuth at all bombarding energies to 450 Mev because of the relative shift of the $f_A(E^*)$ curve for tantalum to higher E^* values. At some higher bombarding energy, beyond the range of the data, we expect the average deposition energy for all inelastic events, which will continue to increase monotonically with bombarding energy, to become greater than the average deposition energy for fission, since the latter may be expected to level off as the branching ratio for fission decreases (see Fig. 6). Figures 9 and 10 also show that, at a given bombarding energy, the average deposition energy for fission is greater than the most probable deposition energy for fission. The values for the average and most probable deposition energies for the 450-Mev fission of bismuth and tantalum obtained in this fashion from excitation-function data, are in very good agreement with the corresponding values obtained from recoil studies at 450 Mev.¹²

The probability for fission as a function of deposition energy E^* for bombarding energy E_p is given by $F_A(E^*, E_p)$. This quantity is plotted as a function of E^* in Fig. 11 for bismuth and tantalum for E_p of 450 Mev. It is apparent that fission occurs over a wide range of deposition energy for both bismuth and tantalum. If it is assumed that fission occurs after de-excitation by evaporation of neutrons, there then is a correspondence between "fissioning nucleus" and deposition energy. The most probable "fissioning nucleus" in the 450-Mev proton bombardment of bismuth has a mass of 191, and gives rise to about 7% of all fissions. The most probable

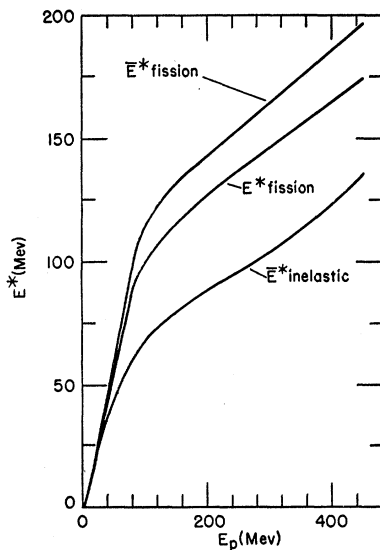


FIG. 10. Variation of deposition energy with bombarding energy for tantalum. \bar{E}^* fission—average deposition energy for fission. E^* fission—most probable deposition energy for fission. \bar{E}^* inelastic—average deposition energy for all inelastic events.

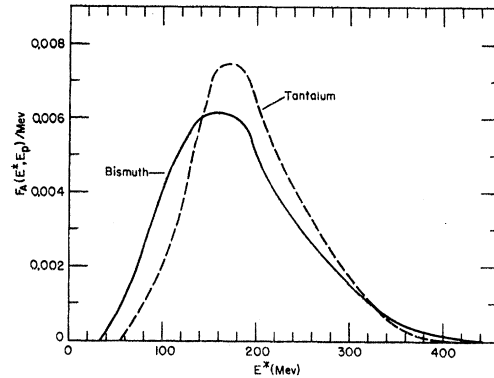


FIG. 11. Variation of $F_A(E^*, E_p)$ with E^* for the fission of bismuth and tantalum with 450-Mev protons.

"fissioning nucleus" for tantalum has a mass of 163, and gives rise to about 8% of all fissions. Previously, more qualitative results on the spread of fissioning nuclei in high-energy fission have been presented by Douthett and Templeton,¹⁸ Biller,¹⁹ and Nervik and Seaborg.¹⁶ We have previously¹² shown that for both bismuth and tantalum fission, the most probable fissioning nucleus gives rise to the most probable fission fragment over most of the fission region. Since the most probable fragments for a given mass have been shown to account for perhaps as much as 40% of the total chain yield,¹¹ we might expect that the most probable fissioning nucleus would give rise to about 40% of the fissions. The fact that instead it only gives rise to 7 or 8% of all fissions implies that there is a set of perhaps 5 to 10 fissioning nuclei, with an average deposition energy that of the most probable fissioning nucleus, which gives rise to the most probable fragments throughout most of the fission region. The variation of $F_A(E^*, E_p)$ for Cu^{67} , a primary fragment in the fission of bismuth, given in Fig. 7, shows about the same variation with deposition energy, or fissioning nucleus, as the total fission process, in agreement with the above view.

VI. CONCLUSION

In this study we have obtained branching ratios for the formation of nuclides at given deposition energies from measured excitation functions and deposition energy spectra obtained from Monte Carlo calculations. These branching ratios were used to analyze the measured cross sections for the formation of products in Bev-proton bombardments of lead into low deposition energy "fission" and high deposition energy "fragmentation" components. For bombarding energies above 1 Bev, the fragmentation process was found to contribute to the observed formation cross sections of nuclides over the mass region conventionally attributed to fission, and to predominate over the fission process

¹⁸ E. M. Douthett and D. H. Templeton, *Phys. Rev.* **94**, 128 (1954).

¹⁹ W. F. Biller, University of California Radiation Laboratory Report, UCRL-2067, December, 1952 (unpublished).

for bombarding energies greater than about 1.5 Bev. At 3-Bev bombarding energy, the mass distribution of fragmentation products exhibits a broad minimum at a mass of about 100, with an increase in yield of about an order of magnitude in going to the lightest and heaviest fragments.

The average and most probable deposition energies for formation of nuclides at given bombarding energies were calculated. The variation with bombarding energy of the average deposition energy for formation of a given nuclide was shown to depend on the nature of the process responsible for the formation of this nuclide. An experimental study of this variation should therefore be of value in the study of formation processes. The fission process for bismuth was compared with that for tantalum. Fission was found to account for a maximum of 17% of the total inelastic cross section of bismuth, this maximum occurring at a deposition energy of 190 Mev, whereas for tantalum the corresponding value is 0.8% at a deposition energy of 230 Mev. The "intrinsic" fissionability of bismuth was found to be 30 times

greater than that of tantalum for 450-Mev bombardments. The average deposition energy for fission of tantalum was found to be greater than that for fission of bismuth for all bombarding energies to 450 Mev. Both deposition energies for fission were greater than the corresponding deposition energies for all inelastic events at bombarding energies above 50 Mev. The most probable "fissioning nucleus" from 450-Mev bombardment of bismuth and tantalum accounts for about 7% of all fissions.

ACKNOWLEDGMENTS

The authors gratefully acknowledge the advice and criticism of Professor Anthony Turkevich and his cooperation in making the results of the Monte Carlo calculations available prior to publication. We are especially grateful to Professor Anthony Turkevich, Dr. Nicholas Metropolis, Dr. Gerhart Friedlander, and Professor J. M. Miller for permission to present the deposition energy spectra from the Monte Carlo calculations prior to publication.

Energy Dependence of the K^+ -Meson Interaction Cross Section*

M. WIDGOTT, *Cyclotron Laboratory, Harvard University, Cambridge, Massachusetts*
 A. PEVSNER, *Department of Physics, The Johns Hopkins University, Baltimore, Maryland*
 D. FOURNET DAVIS,† D. M. RITSON, AND R. SCHLUTER, *Laboratory for Nuclear Science and Engineering, Massachusetts Institute of Technology, Cambridge, Massachusetts*

AND

V. P. HENRI, *Department of Physics, Northeastern University, Boston, Massachusetts*

(Received May 27, 1957)

K^+ interactions in nuclear photographic emulsion have been studied at three effective mean K^+ energies: 54 Mev, 95 Mev, and 140 Mev. The cross section for inelastic interaction is found to increase slightly with energy. The scattering appears to be s -wave, $T=1$, at low energies, with p -wave scattering becoming appreciable above about 100 Mev.

INTRODUCTION

IN order to obtain information on the interaction of K mesons with nucleons, a number of groups have studied the scattering of low-energy K^+ mesons from both hydrogen and heavier nuclei.¹⁻¹⁰ The following,

(1)–(3), are the only possible processes (at energies below meson-production thresholds) in accordance with the requirements of the strangeness scheme, which forbids K^+ absorption. The fact that in no case has absorption been found is in agreement with this prediction.

$$K^+ + p \rightarrow K^+ + p, \quad (1)$$

$$K^+ + n \rightarrow K^+ + n, \quad (2)$$

$$K^+ + n \rightarrow K^0 + p. \quad (3)$$

* The work at Harvard University and the Massachusetts Institute of Technology was assisted by the joint program of the Office of Naval Research and the U. S. Atomic Energy Commission. The work at The Johns Hopkins University was assisted by the Office of Scientific Research of the Air Force.

† Now a Fellow of the American Association of University Women at the University of Rochester.

¹ Lannutti, Chupp, Goldhaber, Goldhaber, Helmy, Iloff, Pevsner, and Ritson, *Phys. Rev.* **101**, 1617 (1956).

² L. S. Osborne, *Phys. Rev.* **102**, 296 (1956).

³ Biswas, Ceccarelli-Fabbrichesi, Ceccarelli, Gottstein, Varshneya, and Waloschek, *Nuovo cimento* **5**, 123 (1957).

⁴ Cocconi, Puppi, Quarenì, and Stanghellini, *Nuovo cimento* **5**, 172 (1957).

⁵ Baldo-Ceolin, Cresti, Dallaporta, Grilli, Guerriero, Merlin, Salandin, and Zago, *Nuovo cimento* **5**, 402 (1957).

⁶ B. Sechi Zorn and G. T. Zorn, *Bull. Am. Phys. Soc. Ser. II*, **2**, 20 (1957).

⁷ Bristol Group (private communication).

⁸ D. Fournet Davis, *Phys. Rev.* **106**, 816 (1957); and Massachusetts Institute of Technology thesis 1957 (unpublished).

⁹ J. E. Lannutti *et al.*, *Proceedings of the Seventh Annual Rochester Conference on High-Energy Physics, 1957* (Interscience Publishers, Inc., New York, 1957).

¹⁰ D. Glaser, *Proceedings of the Seventh Annual Rochester Conference on High-Energy Physics, 1957* (Interscience Publishers, Inc., New York, 1957).